

Λ and Σ potentials in dense matter based on chiral EFT: Bridging heavy-ion collisions, hypernuclei, and neutron stars

Asanosuke Jinno^{1,*}, Koichi Murase², Yasushi Nara³, and Johann Haidenbauer⁴

¹Department of Physics, Faculty of Science, Kyoto University, Kyoto, 606-8502, Japan

²Department of Physics, Tokyo Metropolitan University, Hachioji 192-0397, Japan

³Akita International University, Yuwa, Akita-city 010-1292, Japan

⁴Institute for Advanced Simulation, Forschungszentrum Jülich, D-52425 Jülich, Germany

Abstract. The Λ and Σ directed flows at $\sqrt{s_{NN}} = 4.5$ GeV are investigated to examine their sensitivity to the hyperon single-particle potentials. The single-particle potentials are obtained from G -matrix calculations with two- and three-body forces based on SU(3) chiral effective field theory. The $\Lambda + \Sigma^0$ directed flow shows sensitivity to the variation in the Σ single-particle potential. Its effect is more pronounced for the Σ^0 directed flow.

1 Introduction

A unified approach relating heavy-ion collisions, low-energy nuclear experiments, and neutron stars with the modern nuclear force derived from chiral effective field theory (EFT) has provided valuable insights into the properties of the equation of state of dense matter (e.g. Ref. [1]). For a microscopic description of dense matter, such an approach must be extended to the hyperon sector. A precise understanding of the hyperon single-particle potentials in nuclear matter is essential for addressing the long-standing hyperon puzzle in neutron stars.

In this contribution, we examine the Λ and Σ directed flows at $\sqrt{s_{NN}} = 4.5$ GeV and investigate their sensitivity to the hyperon single-particle potentials [2], obtained from the G -matrix calculations with two- (2BF) and three-body forces (3BF) based on chiral EFT. These potentials are sufficiently repulsive at high densities to solve the hyperon puzzle and have been shown to be consistent with the hypernuclear spectroscopy [3]. We employ a relativistic quantum molecular dynamics (RQMD) model implemented into the Monte-Carlo event generator JAM2¹ with updates since our previous work [4].

As novel feature, we implement the Σ single-particle potential, evaluated from the same hyperon-nucleon (YN) interaction as that of the Λ . In our previous work [4] on the Λ directed flow, all hyperons and their resonances were assumed to feel the same single-particle potential as the Λ . Meanwhile, the Σ^0 contribution should have an impact because the Λ directed flow is in essence the $\Lambda + \Sigma^0$ directed flow due to the process $\Sigma^0 \rightarrow \gamma + \Lambda$. Also, the Σ single-particle potential is expected to be more repulsive compared to that of Λ as reflected in the non-existence of Σ hypernuclei except for ${}^4_{\Sigma}\text{He}$. We discuss the influence of the Σ single-particle potential on the $\Lambda + \Sigma^0$ and the Σ^0 directed flows.

*e-mail: jinno@ruby.scphys.kyoto-u.ac.jp

¹<https://gitlab.com/transportmodel/jam2>

2 Λ and Σ single-particle potentials from chiral EFT

We use the Lorentz-vector version of the relativistic quantum molecular dynamics (RQMDv) model [5] implemented in JAM2, which gives the rapidity dependence of the proton directed flow compatible with the data for a wide range of beam energies $\sqrt{s_{NN}} = 3\text{--}20$ GeV [5].

We employ the Λ and Σ potentials evaluated from 2BFs and 3BFs based on SU(3) chiral EFT. The G -matrix calculation is employed to calculate the single-particle potentials. The 2BF is chosen to be one of the chiral potential from the Jülich-Bonn group, NLO13 [6] with the cutoff of 500 MeV. The 3BF is implemented as an effective density-dependent 2BF in which the low-energy constants (LECs) are estimated via the decuplet-saturation assumption [2, 7]. The LECs involved in the 3BF are determined to fulfill two constraints: $U_{\Lambda}(\rho_0, k = 0) \approx -30$ MeV [8] from the Λ hypernuclear spectroscopy and $U_{\Lambda}(3\rho_0, k = 0) > 80$ MeV in pure neutron matter so that the appearance of Λ 's in neutron stars is suppressed. We choose the set of the 3BF LECs that produces the most repulsive Σ potential.

The Λ and Σ single-particle potentials are implemented in RQMDv by fitting the following forms to the results from chiral EFT:

$$U(\rho, k) = U_{\rho}(\rho/\rho_0) + U_m^0(\rho, k), \quad (1)$$

$$U_{\rho}(u) = au + bu^{4/3} + cu^{5/3}, \quad U_m^0(\rho(x), k) = \frac{C}{\rho_0} \int d^3k' \frac{f(x, k')}{1 + [(k - k')/\mu]^2}, \quad (2)$$

where a, b, c, C and μ are fitting parameters and $f(x, k)$ is the baryon single-particle distribution function. In the actual heavy-ion simulation, we implement the momentum-dependent potential in the Lorentz-vector form U_m^{μ} [4].

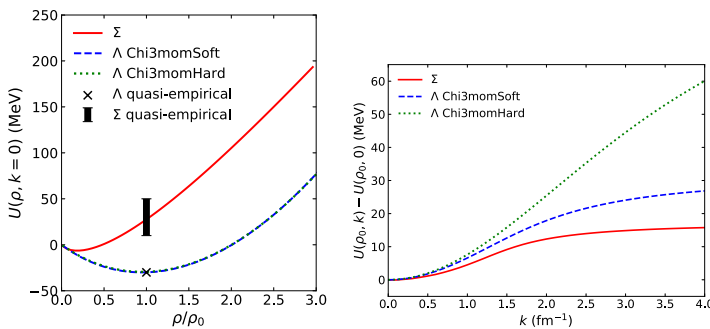


Figure 1. Density dependence (left panel) and momentum dependence (right panel) of the Λ and Σ single-particle potentials in symmetric nuclear matter. The momentum dependence is subtracted by its value at $k = 0$. The single-particle potentials are fitted to the results obtained for two- and three-body forces based on chiral EFT. The solid lines correspond to the Σ single-particle potential. The dashed and dotted lines represent the Λ single-particle potentials with different momentum dependencies above $k > 1 \text{ fm}^{-1}$. The quasi-empirical values at ρ_0 are taken from Ref. [8].

The fitted results for the density dependence of the hyperon single-particle potentials are shown on the left panel of Fig. 1. The Σ single-particle potential is much more repulsive compared to the Λ single-particle potential. This behavior is consistent with the quasi-empirical value inferred from Σ^- atoms and (π^+, K^+) inclusive spectra: $U_{\Sigma}(\rho_0, k = 0) = 30 \pm 20$ MeV [8].

For the momentum dependence, we prepared two scenarios to simulate the uncertainty in chiral EFT. Chi3momHard and Chi3momSoft are constructed to reproduce the chiral EFT result [9] up to $k = 2.5 \text{ fm}^{-1}$ and up to 1.0 fm^{-1} , respectively, as shown on the right panel of Fig. 1. The momenta correspond roughly to the potential cutoff of $\approx 500 \text{ MeV}$ and to 40% of its value. The Σ momentum dependence is constructed by a similar procedure as Chi3momSoft.

3 Λ and Σ directed flows

We consider the rapidity dependence of the hyperon directed flows,

$$v_1 = \langle \cos \phi \rangle = \left\langle \frac{p_x}{\sqrt{p_x^2 + p_y^2}} \right\rangle, \quad (3)$$

where ϕ is the azimuthal angle measured from the reaction plane, and p_x and p_y are the transverse momenta of a particle. The brackets indicate averaging over all events and particles.

Let us mention three updates in JAM2 since our previous work [4]: First, the collision term in the Boltzmann equation is updated to the Poincaré covariant one [10]. Second, the hyperon-nucleon cross section is updated to the ones calculated from the up-to-date chiral force at next-to-next-to-leading order [11]. Third, a new RQMD equation of motion [12] is employed, which provides an accurate simulation of the equation of state, in contrast with the traditional QMD calculations [13, 14]. We have confirmed that these updates have only a subtle impact on the hyperon directed flows. We label the results from the version used in Ref. [4] as RQMDv1 and the new one as RQMDv2.

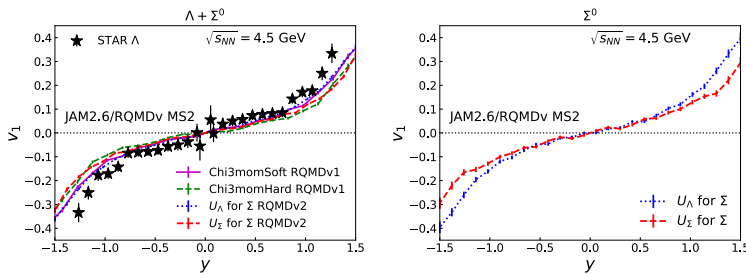


Figure 2. Directed flows of $\Lambda + \Sigma^0$ (left panel) and Σ^0 (right panel) as functions of the rapidity at $\sqrt{s_{NN}} = 4.5 \text{ GeV}$ in the mid-central Au + Au collisions. The STAR data is taken from Ref. [15].

The results of the $\Lambda + \Sigma^0$ directed flow in mid-central Au + Au collisions at $\sqrt{s_{NN}} = 4.5 \text{ GeV}$ are shown on the left panel of Fig. 2 and compared with the STAR data [15]. In the RQMDv1 calculations, a suppression is found in case of the harder momentum dependence, as discussed in our previous study [4]. This illustrates that the harder momentum dependence leads to more repulsive hyperon potentials. Experimental information on the optical potential of Λ would be useful for reducing the model uncertainty. Substituting the Σ single-particle potential for the Λ one results in a similar suppression.

The effect of the Σ potential is more significant for the Σ^0 directed flow than for the $\Lambda + \Sigma^0$ case, where the particle production ratio of Λ/Σ_0 is $R = 3.05$ at $\sqrt{s_{NN}} = 4.5 \text{ GeV}$, as simulated in JAM2. We note that the HADES experiment [16] at $\sqrt{s_{NN}} = 2.55 \text{ GeV}$ report a ratio of $R = 3.2$.

The $\Lambda + \Sigma^0$ and Σ^0 directed flows are useful to determine the repulsion of the Σ single-particle potential, which has larger theoretical uncertainty in their quasi-empirical values [8] compared to Λ potential: $U_\Lambda(\rho_0, k = 0) \approx -30$ MeV [3, 8] and $U_\Sigma(\rho_0, k = 0) = 30 \pm 20$ MeV [8].

4 Summary

We investigated the sensitivity of the Λ and Σ directed flows to the hyperon single-particle potential in dense matter in the mid-central Au+Au collision at a RHIC-BES energy, $\sqrt{s_{NN}} = 4.5$ GeV. The single-particle potentials are obtained from two- and three-body forces based on chiral EFT. The resulting Σ single-particle potential is more repulsive compared to the Λ one. Their values at the saturation density are consistent with the quasi-empirical values [8].

The $\Lambda + \Sigma^0$ directed flow is suppressed when incorporating the Σ single-particle potential. The suppression is of the same magnitude as the uncertainty in the momentum dependence. This effect is more significant for the Σ^0 directed flow itself. The Σ potential has large uncertainty even at the saturation density due to the lack of the Σ hypernuclei except for the special case ${}^4_2\text{He}$. The hyperon directed flows can help to further constrain properties of the Σ single-particle potential.

In this work, the hyperon resonances are assumed to feel the same single-particle potentials as the corresponding ground state hyperons. Their single-particle potentials should be investigated because a number of resonances are produced during the early stage in the collisions and affect the ground-state hyperon observables by the feed-down effect. A work by using a parity-doublet model is ongoing and will be given elsewhere.

AJ would like to thank Dominik Gerstung for kindly sharing his code with us. This work was supported in part by JST SPRING (No. JPMJSP2110) and by the Grants-in-Aid for Scientific Research from JSPS (Nos. JP21K03577, JP25K07284, JP23K13102, and JP25KJ1584).

References

- [1] S. Huth et al., *Nature* **606**, 276 (2022)
- [2] D. Gerstung et al., *Eur. Phys. J. A* **56**, 175 (2020)
- [3] A. Jinno et al., *Phys. Rev. C* **108**, 065803 (2023)
- [4] Y. Nara et al., *Phys. Rev. C* **106**, 044902 (2022)
- [5] Y. Nara et al., *Phys. Rev. C* **105**, 014911 (2022)
- [6] J. Haidenbauer et al., *Nucl. Phys. A* **915**, 24 (2013)
- [7] S. Petschauer et al., *Nucl. Phys. A* **957**, 347 (2017)
- [8] A. Gal et al., *Rev. Mod. Phys.* **88**, 035004 (2016)
- [9] M. Kohno, *Phys. Rev. C* **97**, 035206 (2018)
- [10] Y. Nara et al., *Phys. Rev. C* **108**, 024910 (2023)
- [11] J. Haidenbauer et al., *Eur. Phys. J. A* **59**, 63 (2023)
- [12] Y. Nara et al. (2025), arXiv, 2507.23294
- [13] M. Colonna et al. (TMEP), *Phys. Rev. C* **104**, 024603 (2021)
- [14] J. Xu et al. (TMEP), *Phys. Rev. C* **109**, 044609 (2024)
- [15] J. Adam et al. (STAR), *Phys. Rev. C* **103**, 034908 (2021)
- [16] M. Becker (HADES), *EPJ Web Conf.* **296**, 12002 (2024)